

The Breakdown of Cell Membranes by Electrical and Mechanical Stress

Johannes Akinlaja* and Frederick Sachs#

Departments of *Physics and #Biophysical Sciences, State University of New York, Buffalo, New York 14214 USA

ABSTRACT We attempted to determine whether mechanical tension and electrical stress couple to cause membrane breakdown in cells. Using cell-attached patches from HEK293 cells, we estimated the mechanically produced tension from the applied pressure and geometry of the patch. Voltage pulses of increasing amplitude were applied until we observed a sudden increase in conductance and capacitance. For pulses of 50 μ s duration, breakdown required >0.5 V and was dependent on the tension. For pulses of 50–100 ms duration, breakdown required 0.2–0.4 V and was independent of tension. Apparently two physically different processes can lead to membrane breakdown. We could explain the response to the short, high-voltage pulses if breakdown occurred in the lipid bilayer. The critical electromechanical energy per unit area for breakdown by short pulses was ~ 4 dyne/cm, in agreement with earlier results on bilayers. Our data suggest that, at least in a patch, the bilayer may hold a significant fraction ($\sim 40\%$) of the mean tension. To be compatible with the large, nonlytic area changes of patches, the bilayer appears to be pulled toward the pipette tip, perhaps by hydrophobic forces wetting membrane proteins bound to the glass. Although breakdown voltages for long pulses were in agreement with earlier work on algae, the mechanism(s) for this breakdown remain unclear.

INTRODUCTION

The mechanical properties of eucaryotic cells are complex (Wang and Ingber, 1994). Forces applied to a cell are distributed over many components, including the extracellular matrix, the bilayer, and the cytoskeleton. The latter distributes forces within the cell cortex and as deep as the nucleus (Stamenovic et al., 1996; Ingber et al., 1995; Mooney et al., 1995; Wang and Ingber, 1995). The cytoskeleton consists of many proteins that are dynamically linked and capable of causing complex dynamic responses to an applied force (Small and Morris, 1994; Hamill and McBride, 1992). These responses, in turn, may be modulated by a host of second messengers (Vandeburgh, 1993). The same complex responses may occur in the extracellular matrix, although relatively few data are available. As a result, it is difficult to understand the distribution of forces within a cell membrane.

One approach to decoding the distribution of forces is to use genetics to knock out or modify a particular protein, such as dystrophin, for example (Franco-Obregon and Lansman, 1994; Cox et al., 1993). However, because of the long time scale of these experiments, reequilibration of the dynamically interacting components leads to alterations in others (Campbell and Kahl, 1989) and results cannot be reliably compared to the wild type. Ideally, one would instantaneously remove the element in question and follow the relaxation process, but such tools do not yet exist.

An alternative approach is to exploit physical differences in the cortical components. The one membrane component that can be directly addressed in this way is the lipid bilayer (Dai and Sheetz, 1995) and its elements. (In what follows, we will refer to the bilayer and integral membrane proteins as “the membrane,” as opposed to the larger structure of the “cortex.”) The membrane is distinguishable as the only region over which the transmembrane potential field is significant. If one tests the distribution of stress using an electrical inquiry, one can selectively interrogate the membrane. In this way we attempted to measure how much of the mean cortical stress is borne by the membrane.

Needham and Hochmuth (1989) conducted a series of electromechanical experiments on lipid bilayers that suggested breakdown occurs when the average energy density exceeds a threshold. This energy is the sum of mechanical energy due to the far-field tension thinning the membrane, and electrical energy from the transmembrane field compressing the membrane. We reasoned that we could test whether the membrane of eucaryotic cells was subject to significant tension in a similar manner. If the membrane behaved like a lipid bilayer, and if a significant fraction of the mechanical stress applied to the cell reached the membrane, then the breakdown voltage would be reduced in a predictable manner.

We used the cell-attached patch-clamp configuration and hydrostatic pressure to mechanically stress the patch, and examined the breakdown voltage as a function of mean tension. With 50- μ s pulses, the breakdown voltage was between 500 and >1100 mV and decreased with tension, suggesting that the membrane held a significant amount of the mean tension.

Complicating this interpretation, however, the breakdown voltage with long voltage pulses (100 ms) was independent of tension, although cell membrane breakdown with long voltage pulses ($t > 10$ ms) has also been postulated to arise

Received for publication 8 August 1997 and in final form 7 April 1998.

Address reprint requests to Dr. Frederick Sachs, Department of Biophysics, 120 Cary Hall, SUNY–Buffalo, Buffalo, NY 14214-3005. Tel.: 716-829-3289; Fax: 716-829-2028 or 716-829-3395; E-mail: sachs@fred.med.buffalo.edu.

Dr. Akinlaja's present address is Fakultät für Physik und Astronomie, Universität Würzburg, Am Hubland, 97074 Würzburg, Germany.

© 1998 by the Biophysical Society

0006-3495/98/07/247/08 \$2.00

from the lipids (Teissié and Rois, 1993). For the long pulses, the voltage required for breakdown in our experiments was only 200–400 mV and was tension independent. Apparently the mechanisms of high field/short pulse and low field/long pulse breakdown are fundamentally different.

MATERIALS AND METHODS

Experimental setup and methods

All experiments were carried out with the cell-attached patch clamp at room temperature (26–28°C). To get a clear image of the patch, we used high-magnification differential interference contrast optics with video imaging (Sokabe and Sachs, 1990). Patch pipettes were pulled from thin-walled borosilicate glass (100 λ ; Drummond Scientific) with a Sachs-Flaming micropipette puller (Sutter Instruments), with a seven-step process. In a microforge, the pipettes were bent 1 mm from the tip so that the tip was nearly parallel to the microscope stage (Sokabe and Sachs, 1990). The pipettes were fire polished, and to reduce stray capacitance, the pipettes were coated with Sylgard (Hamill et al., 1981). After fire polishing, the pipette aperture was 1–2 μm in diameter, and the tip resistance was ~ 10 M Ω when filled with normal saline. The pipettes were attached to the headstage of an Axon Instruments patch-clamp amplifier (model 200A, equipped for voltammetry to 1.1 V) with a low-drift holder (Sachs, 1995). Seals ($R > 50$ G Ω) were formed with light mouth suction (< 3 mmHg) at a distance of 4–8 μm from the pipette tip. After seal formation and release of suction, the patch often continued to creep up the pipette until it was 10–15 μm from the tip. The suction (or positive pressure) used to mechanically stress the membrane was applied with a syringe-driven pipette, and the pressure was measured with a semiconductor calibrator (WPI). The voltage pulses used to cause breakdown were applied ~ 20 s after the pressure was set. This delay was needed for the membrane to reach a mechanical steady state (Sokabe et al., 1991).

Because it was unclear whether membrane breakdown in the low voltage range was induced by the same basic process as in the high voltage electrical range, two voltage protocols were used. The high voltage protocol used a series of 50- μs square voltage pulses: the first pulse was 400 mV, and following pulses increased in 50-mV increments. The interpulse delay was 3 s. The low voltage protocol used 50 pulses: the first voltage pulse was 200 mV, and following pulses increased in 25-mV increments. The interpulse delay was 5 s.

Voltage pulses can break down either the patch membrane or the membrane-glass seal. Patch breakdown will give electrical access to the whole cell, resulting in a significant rise in capacitance and hence charging time, whereas seal loss will mainly increase conductance, with little change in capacitance. To distinguish patch breakdown from seal breakdown, we superimposed a 5-mV square wave (60 Hz) on the breakdown pulses and monitored the corresponding currents for changes in conductance and charging time. The voltage-pulse protocols and the recording of the currents were controlled by an Intel PC running routines written in Labview.

Cell preparation

Experiments were performed on human embryonic kidney cells (HEK 293; Auerbach et al., 1996) grown in 89% Dulbecco's minimum essential medium, 10% fetal bovine serum, and 1% penicillin and streptomycin (Gibco). Patch-clamp recordings were performed 2 days after cell passage. The bath solution was (in mM) 140 NaCl, 1.6 KCl, 1 CaCl, 10 HEPES, 10 mannitol. The pipette solution was (in mM) 120 CsF, 10 CsCl, 10 EGTA, 10 HEPES. To improve the visibility of the patch, and to avoid gap junctional communication, we used nonconfluent cells.

Models

Needham and Hochmuth (1989) showed that breakdown of artificial lipid bilayers will occur when the average energy density, \bar{T} , of the membrane

exceeds a critical value, \bar{T}_c . Their equation for \bar{T} is

$$\bar{T} = T + 0.5\epsilon\epsilon_0(V_t/h_c)^2h \quad (1)$$

where T is the average membrane tension, ϵ is the dielectric constant of the membrane, V_t is the transmembrane voltage, h is the thickness of the membrane, and h_c is the "capacitive" thickness of the membrane, which is the thickness, h , of the membrane minus twice the thickness of the lipid headgroups. This may be rewritten as $\bar{T} = T_m + T_e$, where T_m is the tension caused by far-field mechanical stretch and T_e is the tension caused by electrical stress (the electrical energy/area). In Eq. 1, the second term is basically $T_e = C_s V^2/2$; the electrical energy stored in a unit area of membrane with specific capacitance C_s . Although biological membranes are estimated to have specific capacitances of 0.5–1 $\mu\text{F}/\text{cm}^2$ (Hille, 1992; Sokabe et al., 1991), the constants used by Needham and Hochmuth are equivalent to 0.5 $\mu\text{F}/\text{cm}^2$, so we will use this value in what follows. The problem at hand is to determine how T_m depends on the mean far-field tension.

If a patch of membrane is approximated by an isotropic thin spherical shell, the average membrane tension T can be estimated by the Laplace equation:

$$T = 0.5Pr \quad (2)$$

where P is the pressure gradient across the membrane and r is the radius of curvature of the patch. The pressure gradient P was taken to be the difference between the pressure in the pipette and the atmosphere. This assumption ignored any stresses in the cytoplasm attached to membrane and hence should be taken as an overestimate of the actual mean cortical tension. The radius, r , was obtained by fitting a digitized image of the patch to a geometric model (Sokabe et al., 1991). The model assumed that the patch membrane spanned a circular arc between the pipette walls, which were taken to be (locally) straight lines.

Because the voltage pulses were generally hyperpolarizing, the transmembrane potential, V_t , was the sum of the applied voltage and the resting potential of the cell, which was about -40 mV (Auerbach et al., 1996). We did not measure the thickness h of the membrane, the effective thickness h_c , or the dielectric constant ϵ of the membrane. Because the form of the energy function does not depend on the choice of these numbers, we assumed the values to be close to those used by Needham and Hochmuth (1989) ($h \approx h_c \approx 4 \times 10^{-9}$ m, $\epsilon \approx 2.2$).

RESULTS

Electrical pulses either broke the patch membrane, which resulted in an increased charging time (see Fig. 1 and Fig. 2), or the membrane-glass seal, which resulted in no change in charging time (see Fig. 3). A surprising result was that seal loss occurred in the same voltage range as breakdown of the patch and could not be distinguished solely by monitoring the increase of conductance. Although it is possible that a pure increase in conductance might reflect simultaneous breakdown of both the patch and the cell, we never observed the blebs that are characteristic of the formation of large pores in cells when the conductance remains high in the presence of mM Ca^{2+} . Resealing of electrically generated pores in membranes is commonly seen in culture (Zimmermann, 1996), and in cell-attached patches resealing time has been reported to occur within minutes (O'Neill and Tung, 1991). In our experiments, however, we did not observe a significant frequency of resealing after breakdown, so every experiment was carried out on a different cell. The difference in frequency of resealing may simply

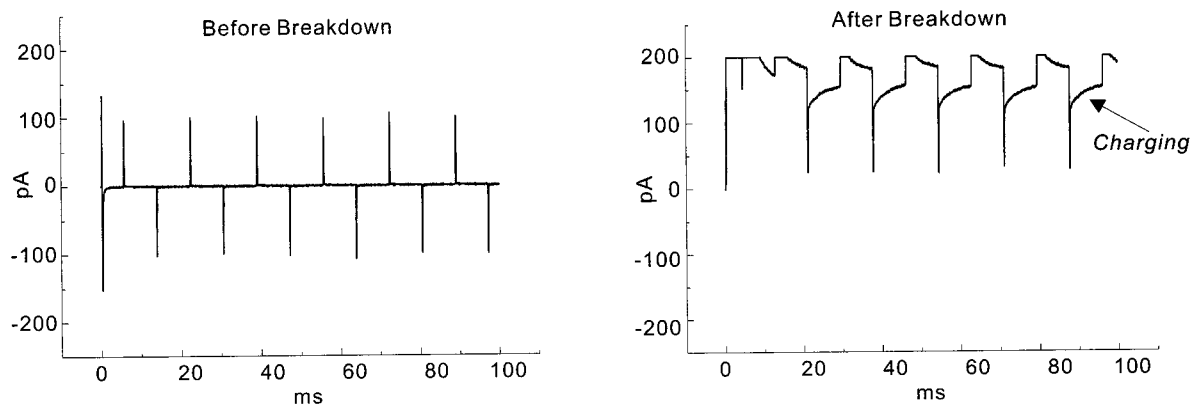


FIGURE 1 Currents for 50- μ s pulses. The current through the patch is plotted as a function of time. A single voltage pulse for membrane rupture was applied at 50 μ s. The seal-test signal was running continuously at 60 Hz and is visible as the train of positive and negative spikes. The left panel is the current before breakdown, and the right panel is the current during breakdown. Notice the increase in charging time with breakdown. The offset in the right panel is due to the resting potential of the cell.

reflect the differences between the heart cells used by O'Neill and Tung and our HEK293 cells.

Our results with 50- μ s pulses (Fig. 4), modeled after the predictions of Needham and Hochmuth (1989), are shown in Fig. 5. Notice that for these pulses, we never observed membrane breakdown in the absence of applied stress, $\bar{T}_m = 0$, with voltages up to the experimental maximum of 1.1 V. This result is in agreement with prior experiments on lipid bilayers, in which breakdown for zero tension never occurred below 1.1 V (Needham and Hochmuth, 1989). Fitting the data of Fig. 5 to the Needham and Hochmuth model gave the following parameters:

$$T_e|_{T=0} = 4.3 \pm 0.4 \text{ dyne/cm}$$

$$\text{slope} = -0.38 \pm 0.07$$

The electrical energy per unit area for breakdown at zero tension, $T_e|_{T=0}$, lies within the range seen for lipid bilayers, 2–30 dyne/cm, depending upon composition (Needham and Nunn, 1990). The scatter in Fig. 4 is probably a result of

sampling a threshold phenomenon, but because the breakdown voltage (Djuzenova et al., 1994) as well as cell deformability (Tsai et al., 1996) are reported to be cell cycle dependent, these factors may contribute as well. However, we did not see a significant variation with cell passage number (data not shown). These results suggest that a significant fraction of the membrane tension is borne by the membrane dielectric, probably the bilayer.

In apparent contradiction to the results above, when we used 100-ms instead of 50- μ s pulses, the breakdown voltage was independent of far-field tension (Fig. 6). Fitting such data to the Needham and Hochmuth equation gives the following parameters:

$$T_e|_{T=0} = 0.47 \pm 0.03 \text{ dyne/cm}$$

$$\text{slope} = -0.004 \pm 0.006$$

Clearly, long and short pulses cause breakdown by different mechanisms, in contradiction to suggestions by Teissié and Rois (1993).

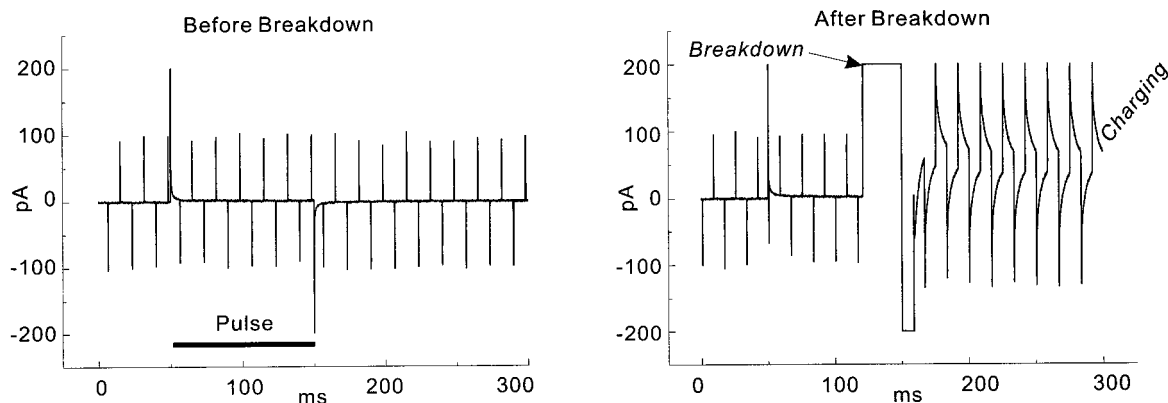


FIGURE 2 Current for 100-ms pulses (notation as in Fig. 1). The 100-ms voltage pulse for breakdown was applied at 50 ms, and is marked by the large spikes at 50 ms and 150 ms. Notice the increase in charging time with breakdown. The offset in the right-hand panel is due to the resting potential of the cell. The spikes in both traces at 60 Hz are caused by the superimposed seal-test signal.

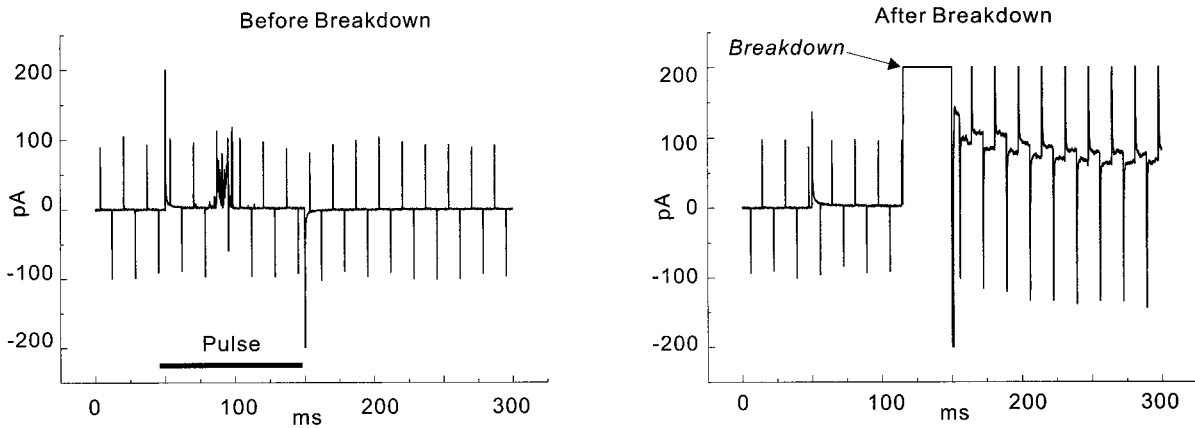


FIGURE 3 Seal loss (notation as Fig. 1). A 100-ms voltage pulse for membrane breakdown was applied at 50 ms, and is marked by the large spikes at 50 ms and 150 ms. No significant increase in charging time is visible—the pulse decay time is fast. A transient burst of increased conductance during the pulse is visible in the left panel.

To examine the influence of deep cytoskeleton on break-down, we separated the membrane from the cytoskeleton, forming a gigasealed bleb within the pipette. To do this, we

first applied positive pressure (>60 mmHg) to push the patch toward the tip, and then slowly decreased the pressure. When the pressure gradient approached zero, the

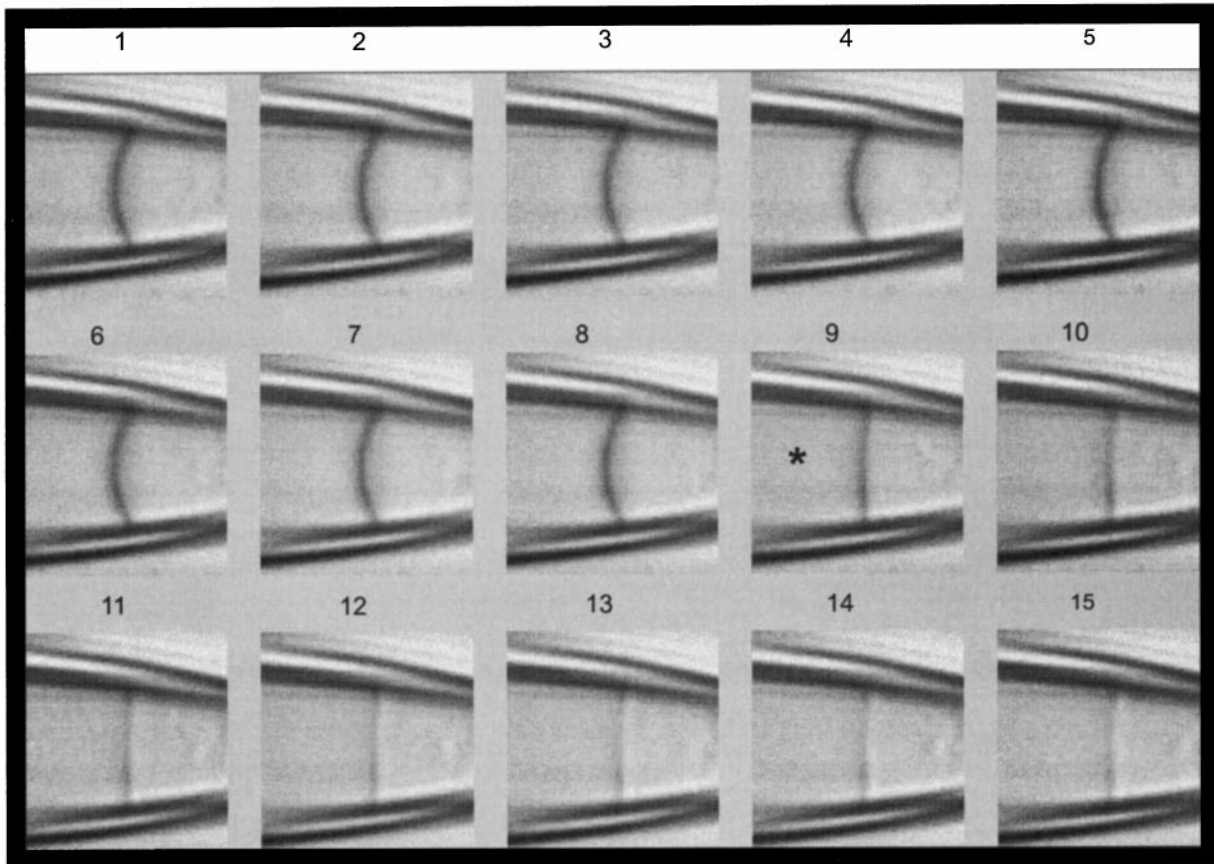


FIGURE 4 Membrane breakdown in a video sequence from left to right and from top to bottom, per frame numbers. The frames are 200 ms apart. The 50- μ s voltage pulse that caused membrane rupture was applied between frames 8 and 9 (marked with an *asterisk*). The loss of the permeability barrier is visible in frame 9 as a flattening of the membrane followed by a loss of contrast, probably due to an influx of saline into the cytoplasm. The sudden flattening after breakdown shows that the current barrier was also the pressure barrier, and that volume forces within the cytoskeleton did not maintain the shape of the patch. Note that the remaining permeabilized “membrane” structure (cytoskeleton plus extracellular matrix) is under resting tension because it is pulled flat.

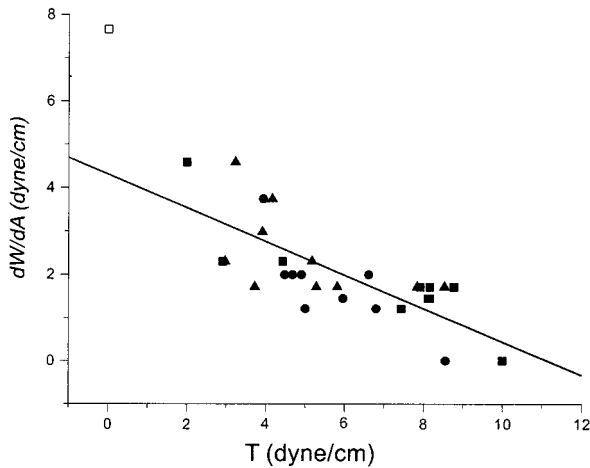


FIGURE 5 High voltage range breakdown compared with predictions of the Needham and Hochmuth model. The electrical energy per unit area for rupture $T_c = dW/dA$ is plotted against the mean mechanical tension T of the patch. The different solid symbol types represent different passages of the cell line, and each symbol represents a different cell. The solid line is the fit to $T_c = Y + XT$, where $Y = 4.3 \pm 0.4$ dyne/cm and $X = -0.38 \pm 0.07$. The open square symbol is the breakdown at zero tension expected from Needham and Hochmuth.

membrane was suddenly sucked up, away from the underlying cytoplasm. This modified membrane had a much lower bending rigidity than the original patch, and showed a rapid strain response to application of pressure, resembling a lipid bilayer (see Fig. 7). As predicted from the high area stiffness of lipid bilayers (100–1500 dyne/cm), the surface area did not change significantly with changes in the pressure gradient (once the patch assumed a spherical shape). Breakdown of this modified membrane occurred at a tension of 3.9 ± 1.3 dyne/cm ($n = 10$). This is approximately the same as the lytic tension we observed for the

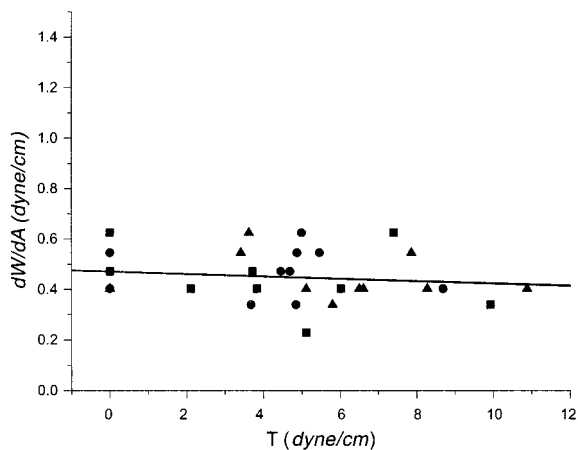


FIGURE 6 Low-voltage, long-pulse breakdown. The electrical energy per unit area to breakdown $T_c = dW/dA_c$ is plotted versus the mean mechanical tension T of the patch. The different solid symbols represent different passages of the cell line, and each symbol represents one cell. The solid line is the fit to $T_c = Y + XT_m$, where $Y = 0.47 \pm 0.03$ dyne/cm and $X = -0.004 \pm 0.006$.

unmodified membrane, suggesting that deeper cortical components do not bear significant stress when suction is applied to the membrane. This conclusion is supported by the fact that breakdown causes a rapid flattening of the patch—removal of the permeability barrier relaxes the curvature of the patch as the pressure gradient is relieved.

However, a significant role of deeper structures is suggested by the surprising result that when we applied strong positive pressures to the patch, it was impossible to break the membrane using 50- μ s pulses up to 1100 mV. According to the Laplace equation, positive or negative pressures should make equal contributions to the stress. This deviation from the thin shell prediction probably arises because when the membrane is pushed into the deeper cortex, the cytoskeleton (possibly reformed under the influence of new stresses; cf. Pender and McCulloch, 1991) begins to support the local stress.

DISCUSSION

The tension dependence displayed in the short pulse data set suggests that the wide scatter of breakdown voltages observed in prior experiments (O'Neill and Tung, 1991) may have been due to the lack of control of membrane tension and/or the inability to know whether the membrane or the seal had broken. Our range of breakdown voltages obtained with short pulses was in agreement with other results on electrical breakdown/electroporation (see Zimmermann, 1996; Weaver and Powell, 1989; for reviews).

If breakdown with 50- μ s pulses is assumed to follow the Needham and Hochmuth model (which was based on pulses of similar duration), the critical electrical energy density at zero tension is equal to the total critical energy density of the membrane, $\bar{T}_c = 4.3 \pm 0.4$ dyne/cm. This is in general agreement with the results on lipid bilayers (Needham and Nunn, 1990) and with the critical energy density, 3.9 ± 1.3 dyne/cm, we found with blebbed membranes.

According to Needham and Hochmuth, the critical energy density does not depend on how the energy is applied to the system. Therefore, for a pure lipid bilayer, the slope of the plot of electrical energy density versus tension (mechanical energy density) should be -1 . In our data, the slope is greater than -1 , as expected if the membrane were mechanically supported by the cytoskeleton and the extracellular matrix, i.e., only a fraction of the applied tension reached the dielectric components of the membrane. The mean tension T in the heterogeneous cellular cortex can be divided into the tension borne by the supporting structures and the tension T_{memb} borne by the membrane dielectric,

$$T_{\text{memb}} = (\bar{T}_c / T_{\text{max}}) T \quad (3)$$

where T_{max} is the far-field tension at which the membrane broke at zero voltage. The slope, $\bar{T}_c / T_{\text{max}} = 0.38 \pm 0.07$, is the fraction of far-field tension borne by the membrane dielectric. This suggests that, at least in a patch, a significant amount of the mean membrane tension is borne by the low

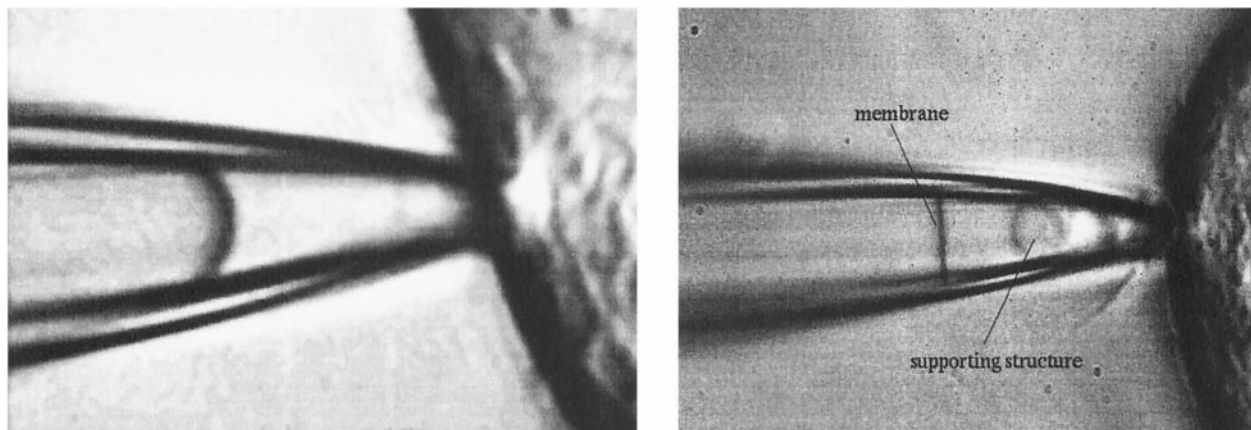


FIGURE 7 Membrane disrupted from the deep cortical cytoskeleton. The left panel shows the patch with positive pressure applied. The right panel shows (on a different patch and lower magnification) release of positive pressure (>60 mmHg); the patch membrane suddenly became dislodged from its supporting structures, stretched flat, and maintained the gigaseal. The patch diameter in the right panel is $3.5 \mu\text{m}$.

dielectric region. This contradicts earlier data from this laboratory, which suggested that essentially all of the (equilibrium) tension is borne by the cytoskeleton (Sokabe et al., 1991). That conclusion was based on the fact that the specific capacitance of the patch appeared to be independent of tension and that the specific capacitance of $0.7 \mu\text{F}/\text{cm}^2$ was similar to that of pure phospholipids. Because the patch had elasticity and hence was not fluid, and we expected that lipids would flow under continued pressure, we presumed that the cytoskeleton alone accounted for the elasticity. This assumption appears to be wrong.

It is clear that the mean patch area can change by $>25\%$ under suction (Fig. 4), but bilayers break down under an area strain of only a few percent (Bloom et al., 1991). Thus the patch itself is much more compliant than the lipids, and the bilayer must have a contour area more than 25% of the patch area. This seems incompatible with the idea that $\sim 40\%$ of the membrane tension is in the lipids. If the bilayer were corrugated as in Fig. 8, Laplace's law would dictate that the bilayer curvature would have to be $\sim 40\%$ of the mean curvature, i.e., we should see a few large bumps in the image of patches (cf. Fig. 4), but the patches appear to be smooth at that level of resolution, and when the membranes break, the resulting patch is planar, not lumpy with excess lipid (Fig. 7). The lipids are not attached at the wall of the pipette at the intersection of the patch with the pipette wall. There is excess lipid, which can be pulled like a fluid sheet through the cytoskeleton and exoskeleton, out of the patch and toward the cell (Fig. 9). This bilayer flows reversibly along the pipette walls under the opposed forces of tension produced by the pressure gradient that pulls the membrane up the pipette, and opposing tension pulling the membrane toward the tip. Such a view is consistent with earlier capacitance data that showed the patch area increased with tension while the specific capacitance was fixed (Sokabe et al., 1991). This view also eliminates the problem of bilayer lysis during large changes in area, because the lytic strain of bilayers is only a few percent. The

forces that draw the bilayer toward the pipette tip are not known. They may be the adhesion forces between the lipids and the glass (Opsahl and Webb, 1994), although it is not clear why these forces should pull toward the tip rather than in any other direction. More likely, the adhesion of the membrane components to the pipette wall have hydrophobic surfaces that attract the lipids.

Regardless of the details, if membrane lipids are under tension during mechanical stress, then it is possible that mechanically sensitive eucaryotic ion channels could be activated by stress in the bilayer. It is known that MscL, a mechanosensitive channel from *Escherichia coli* (Sukharev et al., 1994), works in this fashion (Sachs and Morris, 1998).

Whereas the data obtained with short pulses seem to fit reasonably with the Needham and Hochmuth model, the

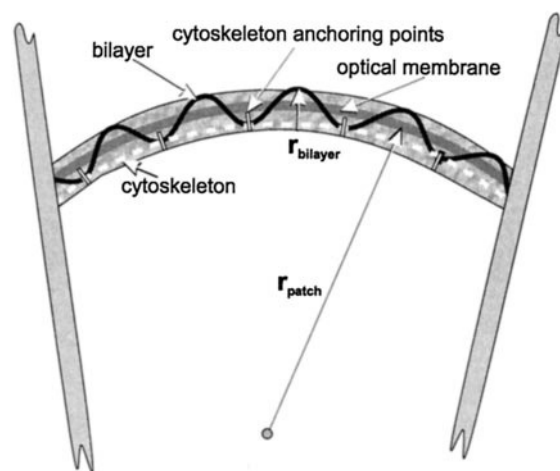


FIGURE 8 Cartoon of the tension-independent breakdown model. In the model, the lipid bilayer bears little tension because the pressure gradient is balanced by a small bending radius. The patch density, as seen in the microscope, is noted as the optical membrane, and has a radius of curvature r_{patch} . The convolutions of the bilayer, maintained by the cytoskeletal anchoring points (integrins?), have a radius r_{bilayer} .

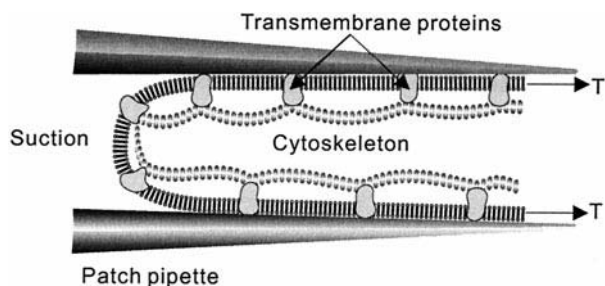


FIGURE 9 Cartoon diagram of a patch in which a fluid bilayer is under resting tension produced by forces (T) exerted parallel to the pipette wall. These forces may arise from lipids solvating the membrane proteins denatured on the glass. A model such as this is required to reconcile the flattening of the membrane after breakdown, the ability to distend the patch beyond the lytic strain of bilayers, the constant specific capacitance of the patch with distension, and the observation that bilayer breakdown (for 50- μ s pulses) is dependent on mean tension in the patch.

data obtained with long pulses were radically different. The voltage required for breakdown decreased to 0.2–0.4 V and was tension independent. Breakdown voltages in this range (320 ± 20 mV) have been observed by Coster (1965) for pseudo-steady-state voltages. It is perhaps significant that when cell populations are subjected to such long-lasting fields, they usually do not recover, i.e., resealing is not observed (Zimmermann, 1996; Weaver and Powell, 1989).

It has been hypothesized that ohmic heating or electrophoresis of membrane proteins is responsible for the long-pulse breakdown (Zimmermann, 1996). However, in our experiments heating can be excluded, because the prebreakdown power for a 10-G Ω patch is <400 pW (0.2 nA $^2 \times 10^{10}$ Ω). If we consider the increase in temperature ν produced by heat Q uniformly developed in a spherical volume of radius a , the maximum increase in temperature is given by $\nu = Q/8\pi aK$, where K is the thermal conductivity (Carslaw and Jaeger, 1959). Although it is devoid of any specific geometric or electrical details, this rough calculation predicts temperature changes of <4 μ C $^\circ$ for objects larger than atomic dimensions. Electrophoretic effects in the plane of the membrane probably cannot account for the difference in behavior for high and low fields, because the electric field in a patch pipette is normal to the membrane (except for the sealing region next to the pipette wall).

In the above analyses, we have assumed that the Needham and Hochmuth model applies to the data obtained with short pulses, but does not apply to the data obtained with long pulses. Let us examine the opposite view: the long pulse data follow Needham and Hochmuth, and the short pulse data do not. For 100-ms pulses, the breakdown voltage was independent of tension. The only way to obtain this effect from a Needham-Hochmuth membrane is to reduce the local radius of curvature so that the applied pressure produces little tension (Fig. 8). The necessary microcorrugations could be produced by the cytoskeleton, e.g., a spectrin-like network. The mechanically induced lysis at zero voltage is then a result of breaking the cytoskeletal links that

caused the corrugations, transferring tension to the bilayer. Voltage-induced breakdown would still be accomplished by breaking the bilayer. However, the critical energies cannot be compared without a model that incorporates time. Breakdown is a threshold behavior, so that fluctuations that reach lytic energy densities are more likely to occur over long times than over short times. The mean electrical energy required to break the membrane in 100 ms is less than that required over 50 μ s. Thus we cannot compare T_c for short and long pulses. The slope of the tension dependence for breakdown with 100-ms pulses is very small (statistically, ~ 0.004 with error limits larger than the mean). However, taking the slope at face value, only 0.4% of the far-field mechanical tension would be expressed in the dielectric, which is consistent with earlier predictions (Sokabe et al., 1991). For a given pressure gradient, the local curvature would be ~ 250 -fold smaller than the patch radius of curvature, or ~ 6 nm for typical patches near lysis. This is even smaller than the order of the cortical cytoskeletal lattice spacing seen in electron micrographs (McGough and Josephs, 1990; Holley and Ashmore, 1990) and appears unrealistic.

We are left in a quandary as to the proper interpretation of the data. What is clear, however, is that the long and short pulse protocols expose two different breakdown mechanisms. It is not known whether such differences in lytic tension are seen in pure lipid bilayers or whether such differences are a property of a heterogeneous biological membrane. If transmembrane proteins denature under voltages that are too small to break the lipids, and this breakdown has a significant delay time, we can account for the results seen with long pulses. Given the agreement of the short pulse breakdown results with results of Needham and Hochmuth, we favor the interpretation that with short pulses we are seeing lipid breakdown, and with long pulses a protein denaturation.

REFERENCES

- Auerbach, A., W. Sigurdson, J. Chen, and G. Akk. 1996. Voltage dependence of mouse acetylcholine receptor gating: different charge movements in di-, mono- and unliganded receptors. *J. Physiol. (Lond.)* 494:155–170.
- Bloom, M., E. Evans, and O. G. Mouritsen. 1991. Physical properties of the fluid lipid-bilayer component of cell membranes: a perspective. *Q. Rev. Biophys.* 24:293–397.
- Campbell, K. P., and S. D. Kahl. 1989. Association of dystrophin and an integral membrane glycoprotein. *Nature*. 338:259–262.
- Carslaw, H. S., and J. C. Jaeger. 1959. *Conduction of Heat in Solids*. Clarendon, Oxford.
- Coster, H. G. L. 1965. A quantitative analysis of the voltage-current relationship of fixed charge membranes and the associated property of “punch-through.” *Biophys. J.* 5:669–686.
- Cox, G. A., N. M. Cole, K. Matsumura, S. F. Phelps, S. D. Hauschka, K. P. Campbell, J. A. Faulkner, and J. A. Chamberlain. 1993. Overexpression of dystrophin in transgenic mdx mice eliminates dystrophic symptoms without toxicity. *Nature*. 364:725–728.
- Dai, J., and M. P. Sheetz. 1995. Mechanical properties of neuronal growth cone membranes studied by tether formation with laser optical tweezers. *Biophys. J.* 68:988–996.

- Djuzenova, C. S., V. L. Sukhorukov, G. Klock, W. M. Arnold, and U. Zimmermann. 1994. Effect of electric field pulses on the viability and on the membrane-bound immunoglobulins of LPS-activated murine B-lymphocytes: correlation with the cell cycle. *Cytometry*. 15:35–45.
- Franco-Obregon, A., Jr., and J. B. Lansman. 1994. Mechanosensitive ion channels in skeletal muscle from normal and dystrophic mice. *J. Physiol.* 481:299–309.
- Hamill, O. P., A. Marty, E. Neher, B. Sakmann, and F. J. Sigworth. 1981. Improved patch-clamp techniques for high resolution current recording from cells and cell-free membranes patches. *Pflügers Arch.* 391:85–100.
- Hamill, O. P., and D. W. McBride, Jr. 1992. Rapid adaptation of single mechanosensitive channels in *Xenopus* oocytes. *Proc. Natl. Acad. Sci. USA.* 89:7462–7466.
- Hille, B. 1992. *Ionic Channels of Excitable Membranes*. Sinauer Associates, Sunderland, MA.
- Holley, M. C., and J. F. Ashmore. 1990. Spectrin, actin and the structure of the cortical lattice in mammalian cochlear outer hair cells. *J. Cell Sci.* 96:283–291.
- Ingber, D. E., D. Prusty, Z. Sun, H. Betensky, and N. Wang. 1995. Cell shape, cytoskeletal mechanics, and cell cycle control in angiogenesis. *J. Biomech.* 28:1471–1484.
- McGough, A. M., and R. Josephs. 1990. On the structure of erythrocyte spectrin in partially expanded membrane skeletons. *Proc. Natl. Acad. Sci. USA.* 87:5208–5212.
- Mooney, D. J., R. Langer, and D. E. Ingber. 1995. Cytoskeletal filament assembly and the control of cell spreading and function by extracellular matrix. *J. Cell Sci.* 108:2311–2320.
- Needham, D., and R. M. Hochmuth. 1989. Electro-mechanical permeabilization of lipid vesicles. *Biophys. J.* 55:1001–1009.
- Needham, D., and R. S. Nunn. 1990. Elastic deformation and failure of lipid bilayer membranes containing cholesterol. *Biophys. J.* 58:997–1009.
- O'Neill, R. J., and L. Tung. 1991. Cell-attached patch clamp study of the electropermeabilization of amphibian cardiac cells. *Biophys. J.* 59:1028–1039.
- Opsahl, L. R., and W. W. Webb. 1994. Lipid-glass adhesion in giga sealed patch-clamped membranes. *Biophys. J.* 66:75–79.
- Pender, N., and C. A. McCulloch. 1991. Quantitation of actin polymerization in two human fibroblast sub-types responding to mechanical stretching. *J. Cell Sci.* 100:187–193.
- Sachs, F. 1995. A low drift micropipette holder. *Eur. J. Physiol.* 429:434–435.
- Sachs, F., and C. Morris. 1998. Mechanosensitive ion channels in nonspecialized cells. In *Reviews of Physiology, Biochemistry and Pharmacology*. M. P. Blaustein, R. Greger, H. Grunicke, R. Jahn, L. M. Mendell, A. Miyajima, D. Pette, G. Schultz, and M. Schweiger, eds. Springer, Berlin. 1–78.
- Small, D. L., and C. E. Morris. 1994. Delayed activation of single mechanosensitive channels in *Lymanea* neurons. *Am. J. Physiol.* 267:C598–C606.
- Sokabe, M., and F. Sachs. 1990. The structure and dynamics of patch-clamped membranes: a study using differential interference contrast light microscopy. *J. Cell Biol.* 111:599–606.
- Sokabe, M., F. Sachs, and Z. Jing. 1991. Quantitative video microscopy of patch clamped membranes stress, strain, capacitance, and stretch channel activation. *Biophys. J.* 59:722–728.
- Stamenovic, D., J. J. Fredberg, N. Wang, J. P. Butler, and D. E. Ingber. 1996. A microstructural approach to cytoskeletal mechanics based on tensegrity. *J. Theor. Biol.* 181:125–136.
- Sukharev, S. I., P. Blount, B. Martinac, F. R. Blattner, and C. Kung. 1994. A large conductance mechanosensitive channel in *E. coli* encoded by MscL alone. *Nature.* 368:265–268.
- Teissié, J., and M. P. Rois. 1993. An experimental evaluation of the critical potential difference inducing cell membrane electropermeabilization. *Biophys. J.* 65:409–413.
- Tsai, M. A., R. E. Waugh, and P. C. Keng. 1996. Cell-cycle dependence of HL-60 cell deformability. *Biophys. J.* 70:2023–2029.
- Vandenburgh, H. H. 1993. Mechanical forces and their second messengers in stimulating growth in vitro. *Am. J. Physiol.* 262:R350–R355.
- Wang, N., and D. E. Ingber. 1994. Control of cytoskeletal mechanics by extracellular matrix, cell shape, and mechanical tension. *Biophys. J.* 66:2181–2189.
- Wang, N., and D. E. Ingber. 1995. Probing transmembrane mechanical coupling and cytomechanics using magnetic twisting cytometry. *Biochem. Cell Biol.* 73:327–335.
- Weaver, J. C., and K. T. Powell. 1989. Theory of electroporation. In *Electroporation and Electrofusion in Cell Biology*. E. Neumann, A. E. Sowers, and C. A. Jordan, editors. Plenum, New York. 111–126.
- Zimmermann, U. 1996. The effect of high-intensity field pulses on eucaryotic cell membranes: fundamentals and applications. In *Electromanipulation of Cells*. U. Zimmermann and G. A. Neil, editors. CRC Press, Boca Raton, FL. 1–106.